



THE STRESS ANALYSIS EFFECT ON STRUCTURAL HEALTH MONITORING IN FUNCTIONALLY GRADED SHELL

Ahmed Raee MADEH ^{1,*}, Nabel Kadum ABD-ALI ^{2,*}

¹ Computer Technical Engineering Department, College of Technical Engineering, The Islamic University, Najaf, Iraq

² Mechanical Engineering Dep., College of Engineering, University of Al-Qadisiyah, Al-Dewaniyah, Iraq.

* Corresponding author, e-mail: ahmed.raee@iunajaf.edu.iq; nabel.abdali@qu.edu.iq

Abstract

The common damage in engineering structures, especially in functionally graded materials, such as failure resulting from fiber breaking or cracking in the matrix or debonding between fibers and matrix, as well as the delamination between the composite material plies and between its layers, may be due to thermal effects, vibration, load concentration as a result of stress and strain for provides information's about structural health monitoring. Virtual energy method such as Hamilton's was used to investigate the effect of the design parameters such as side to thickness and modular as well as material graduation index ratio on the stress-strain relationships, displacement, resultants of stresses, and resultants of mid plane strain. The analysis and simulation of the FGM shells is done in this paper utilizing MATLAB19 code and ABAQUS20 programs. The distribution of characteristics across shell thickness had also been determined using a power law. Normal stress was varied gradually from 5.74 MPa to 9.55 MPa with material index (n) from 0 to 10 respectively, while shear stress varied from 4.2 to 8.23 MPa for the same value of (n). The strain percent increased slightly from 0.00059 to 0.0012 with displacement 0.22 and 1.2 respectively for the same value of (n).

Keyword: health monitoring, FG shell, power and sigmoidal law, virtual energy method, thickness ratio.

1. INTRODUCTION

Many types of damage occur in gradual multi-layers material, as a result of the different properties of these material in each layer that varied through the shell thickness that help to understand the structural health monitoring of shell structural. Functionally graded (FGM) or multi-layers' composite are a type of composite that is inhomogeneous and has mechanical characteristics that change gradually and still through one side to the other. FGM have several benefits over traditional materials, including excellent endurance to significant temperature gradients, reduced stress concentration, greater bonding strength, and etc. As a result, FGM have been widely used in a variety of applications, particularly when considerable temperature differences exist. Moreover, FGM are widely being employed in a variety of applications, including the aviation industry, reactor vessels, space vehicles, electronics, automobiles optics, biomedical engineering and mechanical engineering [1]. Due to material mismatch, stress singularities in such multi-layers composites can develop at the interface between two dissimilar metals. The significantly clear dissimilar in coefficients of thermal properties

will create increase residual strains, especially in a high-temperature condition, such as the engine motor of an air vehicle. As a consequence, the composite can experience cracking or debonding. As a result, the principle of graded shell was established to meet the need conditions of the high-temperature while also eliminating singularities of stress [2]. Multi-phase composite can also create by altering the components of different materials in a specified volume parameter of an essential material. The interfaces between two materials vanish due to the continual change in properties of a multi-phase material, but the properties of two or more separate materials of the composite are conserved. As a result, the stresses singularity at the interfaces of a composite can be reduced, improving strength of bonding. Many studies are trying to improve know order to provide designers with the best possible profile. The change of material characteristics of FGM are often described using a power-law function. The concentrations of strain and stress develop in inter-laminar where the material is continuously but quickly varying in exponential and power functions [3]. Therefore, a sigmoid behavior, consist of twice functions of power law to establish a created volume parameter, and demonstrated that

using a sigmoid function may lower the factors of stress intensity for a fractured structure greatly has been suggested by Jin [4]. The mathematical formulation using the theory of large deformation, Karman for the shell and plates with normal stresses [5]. The structural responses of ceramic-metal composite explored by using a finite element theory which provides for shear stresses [6]. A numerical solution model based on the conventional theory of laminated composite was used to investigate the vibration controlling of multi-layers plates [7]. An elastic branching of plate buckling was investigated with in-plane compressed load employing a combine both structural and micromechanical methods [8]. The meshless collocation technique and the TSDT was used to analyze the static deformations of FGM plate [9]. The transient response of plates and shells has been investigated using radial basis functions and FSDT [10]. Several beam theories (Reddy-Bickford, Timoshenko and Euler-Bernoulli) was used to examine the elasto-static responses of FG plates [11]. Mesh-free moving Kriging (MK) and First Shear Deformation was used to investigate the vibration with bending in multi-layers composite without the use of factors for shear correction [12]. A three-dimensional iso-geometric analysis was used to examine the mechanical behaviors of laminated plates [13]. The formulation within thermal elasticity approach was utilized to investigate the flexural response of FG plates with thermal load [14]. A theoretical framework with finite element models based on the implementation graded plate theory's 3rd shear deformation was developed to examine the buckling behavior of these structures [15]. A numerical solution was applied to explore the free vibration of power distributed over length and thickness of the beam [16-17]. For nonlinear free flexural vibrations, eight-node rectangular elements were used [18]. The in-plane shear stress, direct stress, displacement and transverse stress of a simply supported rectangular shell are examined [19]. The arrangement of fibers reinforced polymeric material in automobile composite bumper has been analyzed [20]. Levy type approach with theory of first shear deformation was utilized to examine the response of buckling load with cross-ply composite shallow shells [21]. The characteristics of a composite material composed of resin strengthened with wasted fiber of glass reinforced pipe (GRP) [22].

The present work focused on the influence of the design constraints such as length to thickness and modular as well as material graduation index ratio on the stress-strain analysis, displacement of a functionally graded shell to detect the weakest regions in those engineering structures and to strength and support these regions in order to ensure the structural health monitoring of shell structural.

2. MATHEMATICAL MODELING

Material properties that are distinct along the formulations of the power law P is different by the thickness of the plate [23]:

$$P(z) = (P_t - P_b)V + P_b, \quad V = \left(\frac{z}{h} + \frac{1}{2}\right)^n \quad (1)$$

Where P_b and P_t denote the properties of the bottom and top surfaces, V represent the volume fraction, h shell thickness, z distance from base and n denotes the material variance profile through the thickness, where n equal to zero for entirely ceramic plates. The direct stresses throughout the direction of thickness may be omitted since the thickness is estimated to be in the limit of 1/20 to 1/100 of its length [20].

In multi-layer plates, the fundamental equations of motion and finite element models created for classical and First-order theory are appropriate. The plate stiffness were assigned by [24]:

$$(A_{ij}, B_{ij}, D_{ij}) = \int_{-\frac{h}{2}}^{\frac{h}{2}} Q_{ij}(z)(1, z, z^2) dz \quad (2)$$

$$(i, j = 1, 2, 6)$$

$$A_{ij} = \int_{-\frac{h}{2}}^{\frac{h}{2}} Q_{ij}(z) dz \quad (i, j = 4, 5) \quad (3)$$

$$(I_0, I_1, I_2) = \int_{-\frac{h}{2}}^{\frac{h}{2}} \left[(\rho_c - \rho_m) \left(\frac{2z+h}{2h} \right) + \rho_m \right] (1, z, z^2) dz \quad (4)$$

$$(i, j = 1, 2, 6)$$

$$Q_{11} = Q_{22} = \frac{E(z)}{1-\nu^2} \quad (5)$$

$$Q_{12} = Q_{21} = \frac{\nu E(z)}{1-\nu^2} \quad (6)$$

$$Q_{44} = Q_{55} = Q_{66} = \frac{E(z)}{2(1+\nu)} \quad (7)$$

for ceramic (c) and metal (m) and modulus, the coefficients of thermal effect as well as the elastic Q_{ij} coefficients, vary with plate thickness [25].

In addition, the energies can be illustrated as [20]:

$$U_e = \iiint \sigma_{ij} \varepsilon_{ij} \delta dx dy dz \quad (8)$$

$$T_e = \frac{1}{2} \iint \rho h w^2 dx dy \quad (9)$$

The minimal potential and kinetic energy concept was used to create mass and stiffness [26]:

$$[K_e] = \int [B]^T [D] [B] dv \quad (10)$$

$$[B]^T = z \left[\frac{\partial^2}{\partial x^2} \quad \frac{\partial^2}{\partial y^2} \quad 2 \frac{\partial^2}{\partial x \partial y} \right] [N]^T \quad (11)$$

and

$$[M_e] = \int [N]^T [\rho] [N] dv \quad (12)$$

The equation of motion calculated as [27]:

$$\int_{t_1}^{t_2} (U_e - T_e + W_e) dt = 0 \quad (13)$$

The stress-strain relationship:

$$\sigma = C \varepsilon \quad (14)$$

The multi-layers materials may be represented using only 21 constants [28].

The constants Q may be represented in terms of engineering coefficient and the relations of stress-strain are given by [29]:

$$\sigma_1 = \frac{E(z)}{(1-2\nu)(1+\nu)} \left[(1-\nu) \frac{\partial u}{\partial x} + \nu \left(\frac{\partial v}{\partial y} + \frac{\partial w}{\partial z} \right) \right] \quad (15)$$

$$\sigma_2 = \frac{E(z)}{(1-2\nu)(1+\nu)} \left[(1-\nu) \frac{\partial v}{\partial y} + \nu \left(\frac{\partial u}{\partial x} + \frac{\partial w}{\partial z} \right) \right] \quad (16)$$

$$\sigma_3 = \frac{E(z)}{(1-2\nu)(1+\nu)} \left[(1-\nu) \frac{\partial w}{\partial z} + \nu \left(\frac{\partial u}{\partial x} + \frac{\partial v}{\partial y} \right) \right] \quad (17)$$

$$\tau_{12} = G(z) \left(\frac{\partial u}{\partial x} + \frac{\partial v}{\partial y} \right) \quad (18)$$

$$\tau_{13} = G(z) \left(\frac{\partial u}{\partial x} + \frac{\partial w}{\partial z} \right) \quad (19)$$

$$\tau_{23} = G(z) \left(\frac{\partial v}{\partial y} + \frac{\partial w}{\partial z} \right) \quad (20)$$

3. NUMERICAL SOLUTION

Finite element method was used to evaluate main equations in this section of the study. Here, a finite element with a conventional discretization method is employed to get numerical results. Partition the complete domain into N equal-length components. The issue is turned into N algebraic equations once FEM is used.

The FGM characteristics can change with direction of thickness, and even the model will involve of multiple layers to provide this properties difference as illustrated in tables (1-2) and figure (1). The characteristics are assessed from bottom utilizing the different rules for volume distribution. The study and simulation of multi-phase composite shell is accomplished in this work utilizing the ABAQUS program. In the modelling of gradient materials, ABAQUS suggests adding additional elements to choose from them. The mechanical loads were applied to the FGM characteristics on a square shell.

Table 1. FG properties of layers.

| | Ply Name | Region | Material | Thickness | CSYS |
|---|----------|----------|----------|-----------|---------|
| 1 | ✓ Ply-1 | (Picked) | AL2O3 | 0.002 | <Layup> |
| 2 | ✓ Ply-2 | (Picked) | GF 0/90 | 0.005 | <Layup> |
| 3 | ✓ Ply-3 | (Picked) | CF 0 | 0.003 | <Layup> |
| 4 | ✓ Ply-4 | (Picked) | GF 0/90 | 0.005 | <Layup> |
| 5 | ✓ Ply-5 | (Picked) | GF 0 | 0.003 | <Layup> |

Table 2. Orientation angles of FG layers.

| Material | Thickness | Orientation Angle | Integration Points | Ply Name |
|----------|-----------|-------------------|--------------------|----------|
| AL2O3 | 0.002 | 0 | 3 | 1 |
| GF 0/90 | 0.005 | 0/90 | 3 | 2 |
| CF 0 | 0.003 | 0 | 3 | 3 |
| GF 0/90 | 0.005 | 0/90 | 3 | 4 |
| GF 0 | 0.003 | 0 | 3 | 5 |

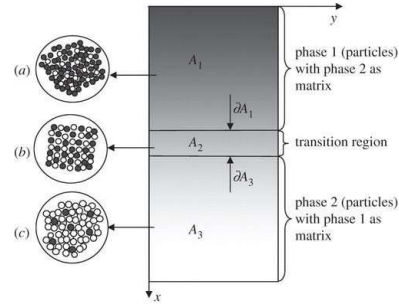


Fig. 1. Thickness variation in each layer [30].

The simply supported edges conditions, as illustrated in figure 2, that is under a uniform pressure.

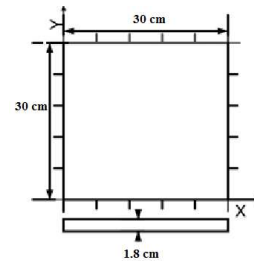


Fig. 2. Rectangular shell dimensions.

4. RESULTS AND DISCUSSIONS

Consider a rectangular elastic plate or shell, the coordinates x and y are determined at the thick of shell's, while the third axis (z), which commenced in the shell central surface is actually in thickness. Top and bottom faces have separate properties as elastic modulus, lateral to longitudinal deformation.

Figures (3) and (4) demonstrate the two power law functions (Power and sigmoidal law).

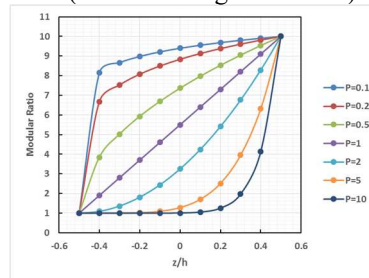


Fig. 3. Power law function (P-FGM).

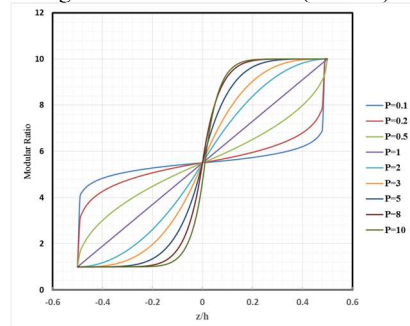


Fig. 4. Sigmoidal law function (S-FGM).

Table 3 shows the stress values of a power function. With modular ratio 2 as illustrated, when

the shell rigidity increases, the stress increases because as material changes from metal matrix to rich ceramics.

Table 3. Effect of power functionally graded shell on structural responses (stresses and displacement).

| Mat. grad. index (n) | Stress (MPa) | Shear xy (MPa) | Strain % | Disp. (mm) |
|----------------------|--------------|----------------|----------|------------|
| 0 (metal) | 5.74 | 4.2 | 0.00059 | 0.22 |
| 0.2 | 6.12 | 4.83 | 0.00062 | 0.25 |
| 0.5 | 6.65 | 5.25 | 0.00066 | 0.292 |
| 1 | 7.28 | 5.8 | 0.00071 | 0.315 |
| 2 | 8.2 | 6.62 | 0.00075 | 0.58 |
| 5 | 8.63 | 7.11 | 0.00085 | 0.72 |
| 8 | 9.24 | 7.32 | 0.001 | 0.92 |
| 10 | 9.55 | 8.23 | 0.0012 | 1.2 |

Many researches have followed the contexts of modifying the contents of polymeric recipes to improve mechanical, physical and chemical properties to suit various engineering applications and achieve the desired work goals [31-32].

5. STATIC STRUCTURAL ANALYSIS

The meshing and element shape of square shell was illustrated in figure (5), in addition to applied loading as shown in figure (6). As even the power index increases, so would the magnitude of deflection. Normal and shear deformation may have the effect of increasing deflection, as predicted. The variations in deformation amounts indicated by the present model are considerable when the thickness ratios is small.

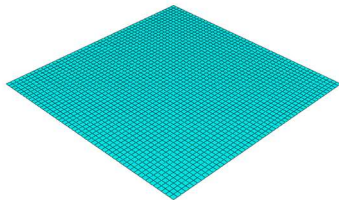


Fig. 5. Meshing type.

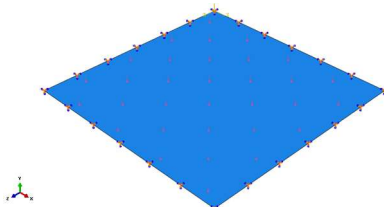


Fig. 6. Loading distribution with boundary conditions.

Figure 7 illustrates the change of the stresses and displacement (structural responses) values with material graduation exponents at various function distributions. As showed, different functions result in various behaviors when the material exponent is increased. When the material graduation exponent is increased with a power and symmetric power with a metal core. In the case of sigmoid function, the stress rises is minimal in the fluctuation of graduation

exponent. Therefore, as the material parameter is increased, the symmetric power with such a ceramics core, as well as the stress, decreases significantly. This tendency is exhibited as the amount of ceramics component with material exponent's decreases.

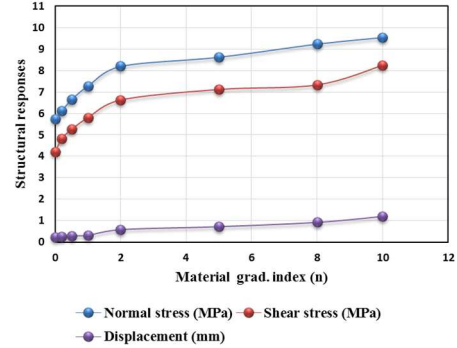


Fig. 7. Power FG shell with structural responses.

Some research has shown the sensitivity of polymeric formulations to several properties such as tensile, hardness and compressive property, in addition to withstanding under high temperature conditions [33-34].

The contour distribution of normal stresses in (σ_1), (σ_2) direction, shear stress (σ_{12}), Von Misses, Tresca stresses and displacement for different length to thickness ratio ($L/t = 10$ and 50) with uniform distribution loading for P-FGM were shown in figures (8) to (19). The geometrical specifications and material characteristics was employed in the present work. Model only one quarter of the domain using a uniform mesh and the biaxial symmetric.

Because Von Misses stress is associated towards the bending moment, which is highest at this support, the largest value for stress was observed there. Between the present and reported results, there is a strong agreement. The results show that the existing formulation behaves very well in order to improve accuracy.

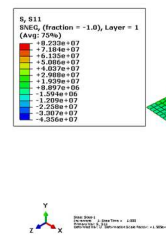


Fig. 8. Normal stress (σ_1) distribution for ($L/t=10$).

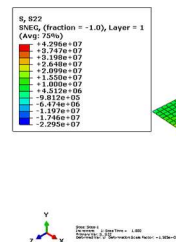


Fig. 9. Normal stress (σ_2) distribution for ($L/t=10$).

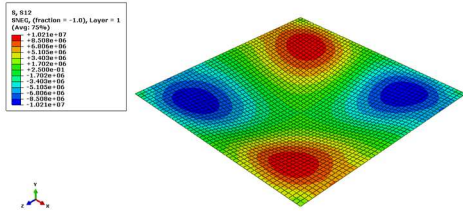


Fig. 10. Shear stress (σ_{12}) distribution for ($L/t=10$).

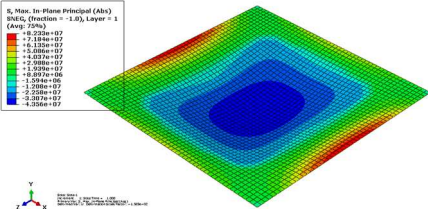


Fig. 11. Von Mises stress distribution for ($L/t=10$).

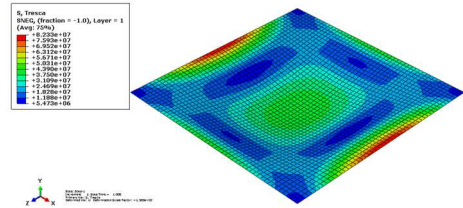


Fig. 12. Tresca stress distribution for ($L/t=10$).

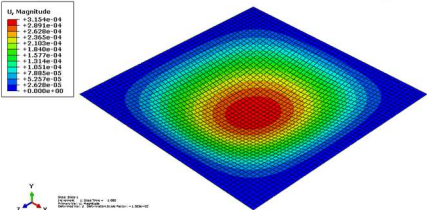


Fig. 13. Displacement distribution for ($L/t=10$).

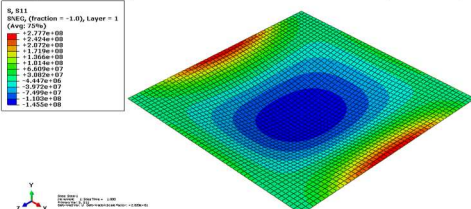


Fig. 14. Normal stress (σ_1) distribution for ($L/t=50$).

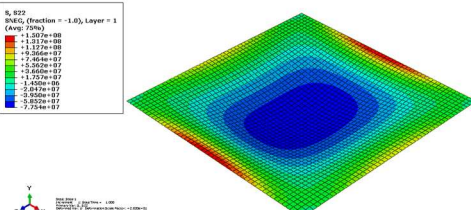


Fig. 15. Normal stress (σ_2) distribution for ($L/t=50$).

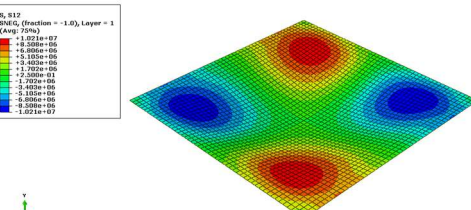


Fig. 16. Shear stress (σ_{12}) distribution for ($L/t=10$).

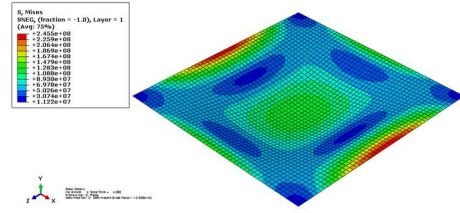


Fig. 17. Von Mises stress distribution for ($L/t=50$).

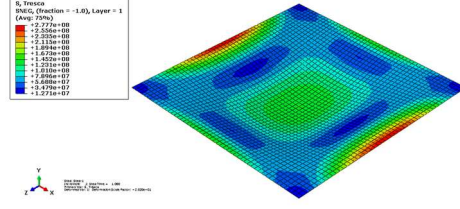


Fig. 18. Tresca stress distribution for ($L/t=50$).

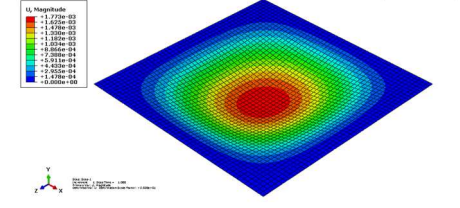


Fig. 19. Displacement distribution for ($L/t=50$).

The potential energy stored in a structure is known as strain energy, also known as deformation energy. The work performed by externally applied load is converted to elastic strain energy, which is stored in the material during the deformation process. When the external load and deformation are gradually reduced, the structure will release a portion from its energy and work, which is known as elastic deformation energy.

Several studies concentrated on the production technique of composite with various attributes as well as engineering disciplines understand the mechanical characteristics of all these components and enhance their characteristics [20-23]. To enhance different applications, the current study intends to employ novel reinforcement materials with different layer arrangements.

6. CONCLUSIONS

The following are some of the results that may be derived from this investigation:

1. The present work introduced the effectiveness of a number of failure theories such as Von-Mises and Tresca in enhancing information about structural health monitoring of shell structural.
2. The structural analysis of functionally gradient structures, which is based on stress and strain analysis, can predict the emergence of regions where damage occurs, which are considered regions of failure in the future.
3. When a multi-layers under a transverse loading, the bottom part of a shell is subjected to much higher stress than the top part; as a result, it is critical to construct the multi-phase composite

with a higher elastic modulus at base to resist fracture.

4. The sigmoidal function offers exceptional in terms of stress intensity. For bending stress and strain, for both mathematical, also the numerical model presented considerable and accurate finding.
5. The elastic ratio has same influence (increasing) on the stresses and displacement for any material distribution function, according to the results.
6. It was demonstrated that by modifying the core properties, stress distributions at the interface between both the face panels and core may be reduced.

Author contributions: *research concept and design, A.R.M.; Collection and/or assembly of data, A.R.M.; Data analysis and interpretation, N.K.A.-A.; Writing the article, N.K.A.-A.; Critical revision of the article, N.K.A.-A.; Final approval of the article, N.K.A.-A..*

Declaration of competing interest: *The authors declare that they have no known competing financial interests or personal relationships that could have appeared to influence the work reported in this paper.*

References

1. Almitani KH. Buckling behaviors of symmetric and antisymmetric functionally graded beams. *Journal of Applied and Computational Mechanics*. 2018;4(2): 115-124. <https://dx.doi.org/10.22055/jacm.2017.23040.1147>.
2. Chi SH, Chung YL. Mechanical behavior of functionally graded material plates under transverse load—Part I: Analysis. *International Journal of Solids and Structures*. 2006;43(13):3657-3674. <https://doi.org/10.1016/j.ijsolstr.2005.04.011>
3. Khor KA, Gu YW, Dong ZL, Srivatsan TS. Plasma Spraying of Functionally Graded NiCoCrAlY/Yttria Stabilized ZrO₂ Coatings Using Composite Powders. ASME International Mechanical Engineering Congress and Exposition. 1997;18343:89-105.
4. Jin ZH, Paulino GH. Transient thermal stress analysis of an edge crack in a functionally graded material. *International Journal of Fracture* 2001;107(1):73-98.
5. Chung YL, Chi SH, The residual stress of functionally graded materials. *Journal of the Chinese Institute of Civil and Hydraulic Engineering*. 2001;13:1-9.
6. Woo J, Meguid SA. Nonlinear analysis of functionally graded plates and shallow shells. *International Journal of Solids and Structures*. 2001;38(42-43):7409-7421.
7. Praveen GN, Reddy JN. Nonlinear transient thermoelastic analysis of functionally graded ceramic-metal plates. *International Journal of Solids and Structures*. 1998;35:4457-4476.
8. He XQ, Ng TY, Sivashanker S, Liew KM. Active control of FGM plates with integrated piezoelectric sensors and actuators. *International Journal of Solids and Structures*. 2001;38:1641-1655. [https://doi.org/10.1016/S0020-7683\(00\)00050-0](https://doi.org/10.1016/S0020-7683(00)00050-0)
9. Feldman E, Aboudi J. Buckling analysis of functionally graded plates subjected to uniaxial loading. *Composite Structures*. 1997;3: 29-36.
10. Ferreira AJM, Batra RC, Roque CMC, Qian LF, Martins PALS. Static analysis of functionally graded plates using third-order shear deformation theory and a meshless method. *Composite structures* 2005;69(4):449-457. <https://doi.org/10.1016/j.compstruct.2004.08.003>.
11. Roque CM, Ferreira AJ, Neves AM, Fasshauer GE, Soares CM, Jorge RMN. Dynamic analysis of functionally graded plates and shells by radial basis functions. *Mechanics of Advanced Materials and Structures*. 2010;17(8):636-652. <https://doi.org/10.1080/15376494.2010.518932>.
12. Karamanli A. Bending behaviour of two directional functionally graded sandwich beams by using a quasi-3d shear deformation theory. *Composite structures*. 2017;174:70-86. <https://doi.org/10.1016/j.compstruct.2017.04.046>.
13. Vu TV, Nguyen NH, Khosravifard A, Hematiyan MR, Tanaka S, Bui TQ. A simple FSDT-based meshfree method for analysis of functionally graded plates. *Engineering Analysis with Boundary Elements*. 2017; 79:1-12. <https://doi.org/10.1016/j.enganabound.2017.03.002>.
14. Tan P, Nguyen-Thanh N, Rabczuk T, Zhou K. Static, dynamic and buckling analyses of 3D FGM plates and shells via an isogeometric-meshfree coupling approach. *Composite Structures*. 2018;198:35-50. <https://doi.org/10.1016/j.compstruct.2018.05.012>.
15. Sator L, Sladek V, Sladek J. Bending of FGM plates under thermal load: classical thermoelasticity analysis by a meshless method. *Composites Part B: Engineering*. 2018;146:176-188. <https://doi.org/10.1016/j.compositesb.2018.04.004>.
16. Reddy JN. Analysis of functionally graded plates, *International Journal for Numerical Methods in Engineering*. 2000;47(1-3):663-684.
17. Alshorbagy AE, Eltaher MA, Mahmoud FF. Free vibration characteristics of a functionally graded beam by finite element method. *Applied Mathematical Modelling*. 2011;35(1):412-425. <https://doi.org/10.1016/j.apm.2010.07.006>.
18. Gilewski W, Pelczyński J. Material-oriented shape functions for fgm plate finite element formulation. *Materials*. 2020;13(3):803. <https://doi.org/10.3390/ma13030803>.
19. Liew KM, He XQ, Ng TY, Sivashanker S. Active control of FGM plates subjected to a temperature gradient: modelling via finite element method based on FSDT. *International Journal for Numerical Methods in Engineering*. 2001;52(11):1253-1271.
20. Abd-Ali NK, Madeh AR. Structural analysis of functionally graded material using sigmoidal and power law. *Diagnostyka*. 2021;22(4):59-65. <https://doi.org/10.29354/diag/14417>.
21. Abd-Ali NK, Madeh AR. Effect of fiber orientation angles on mechanical behavior of car bumper composite. *Kufa Journal of Eng*. 2016;7(3):27-37.
22. Madeh AR, Majeed WI. Effect of boundary conditions on thermal buckling of laminated composite shallow shell. *Materials Today: Proce*. 2021;42:2397-2404. <https://doi.org/10.1016/j.matpr.2020.12.501>.
23. Abd-Ali NK, Madeh AR. Investigation of mechanical properties for unsaturated polyester-based fibre glass composites filled by recycled milled composites. In *IOP Conference Series: Materials Science and Eng*. 2021;1:012129. <https://doi.org/10.1088/1757-899X/1094/1/01212>.

24. Benyamina AB, Boudierba B, Saoula A. Bending response of composite material plates with specific properties, case of a typical FGM “ceramic/metal” in thermal environments. *Periodica Polytechnica Civil Eng.* 2018;62(4):930-938. <https://doi.org/10.3311/PPci.11891>.
25. Chen Y, Jin G, Zhang C, Ye T, Xue Y. Thermal vibration of FGM beams with general boundary conditions using a higher-order shear deformation theory. *Composites Part B: Eng.* 2018;153:376-386. <https://doi.org/10.1016/j.compositesb.2018.08.111>.
26. Reddy JN, Chin CD. Thermomechanical analysis of functionally graded cylinders and plates. *Journal of thermal Stresses.* 1988;21(6):593-626.
27. Evran S. Bending stress analysis of axially layered functionally graded beams. *Ömer Halisdemir Üniversitesi Mühendislik Bilimleri Dergisi.* 2018;7(1): 390 -398.
28. Ashrafi HR, Beiranvand P, Aghaei MZ, Jalili DD. modal analysis of FGM olates (Sus304/Al2O3) using FEM. *Bioceram Dev Appl.* 2018;8(112):2.
29. Fatoni NF, Park WR, Kwon OH. Mechanical property evaluation of functionally graded materials using two-scale modeling. *Journal of the Korean Society of Marine Engineering.* 2017;41(5):431-438.
30. Das S, Das S, Nampi T, Roy K. *Functionally Grade Composite Material Production..2021*
31. Abd-Ali NK, Farhan MM, Hassan NY. Improvement of mechanical properties of the rubbery part in cement packing system using new rubber materials. *Journal of Engineering Science and Technology.* 2021;16(2): 1601–1613
32. Abd-Ali NK, The effect of cure activator zinc oxide nanoparticles on the mechanical behavior of polyisoprene rubber. *Journal of Engineering Science and Technology.* 2020;15(3):2051–2061.
33. Abd-Ali, NK, A new reinforcement material for rubber compounds (Sediment dust nanoparticles and white ceminte). 1st International Scientific Conference of Engineering Sciences- 3rd Scientific Conference of Engineering Science, ISCES 2018 - Proceedings, 2018: 163–168.
34. Farhan MM, Abd-Ali NK, Hassan NY. Development the performance of the rubbery discharge part in flexo-pump system. *Journal of Engineering and Applied Sciences.* 2018;13(24):10148–10157.



Prof. Dr. Nabel Kadum ABD-ALI, received his PhD degree in applied mechanics in 2013 from the University of Technology/Baghdad. He is a teacher in the department of Mechanical engineering in the University of Al-Qadisiyah, Iraq. Research topics: composite materials, rubber technology, polymer engineering, mechanical behaviour of materials.

Received 2022-04-08
Accepted 2022-07-18
Available online 2022-07-21



Ahmed Raee MADEH, PhD student in Applied Mechanics at university of Baghdad, Formal lecturer in computer Engineering Techniques, The Islamic university, Iraq, Research topics: Vibration, stress analysis, Analytical solution.